Automatic Detection of B-lines in In-Vivo Lung Ultrasound

Moshavegh, Ramin; Hansen, Kristoffer Lindskov; Moller-Sorensen, Hasse; Nielsen, Michael Bachmann; Jensen, Jørgen Arendt

Published in:
IEEE Transactions on Ultrasonics, Ferroelectrics, and Frequency Control

Link to article, DOI:
10.1109/TUFFC.2018.2885955

Publication date:
2019

Document Version
Peer reviewed version

This article has been accepted for publication in a future issue of this journal, but has not been fully edited. Content may change prior to final publication. Citation information: DOI 10.1109/TUFFC.2018.2885955, IEEE Transactions on Ultrasonics, Ferroelectrics, and Frequency Control

Automatic Detection of B-lines in *In-Vivo* Lung Ultrasound

Ramin Moshavegh*†, Kristoffer Lindskov Hansen‡, Hasse Møller-Sørensen§,
Michael Bachmann Nielsen‡, and Jørgen Arendt Jensen†
*BK Ultrasound, Mileparken 34, 2730 Herlev, Denmark
†Center for Fast Ultrasound Imaging, Dept. of Elec. Eng., Technical University of Denmark, Lyngby, Denmark
‡Dept. of Diagnostic Radiology, Copenhagen University Hospital, DK-2100 Copenhagen, Denmark
§Dept. of Cardiothoracic Anesthesiology, Copenhagen University Hospital, DK-2100 Copenhagen, Denmark

***Abstract*—This paper proposes an automatic method for accurate detection and visualization of B-lines in ultrasound lung scans, which provides a quantitative measure for the number of B-lines present. All the scans used in this study were acquired using a BK3000 ultrasound scanner (BK Ultrasound, Denmark) driving a 5.5 MHz linear transducer (BK Ultrasound). Four healthy subjects and four patients after major surgery with pulmonary edema, were scanned at four locations on each lung for B-line examination. Eight sequences of 50 frames were acquired for each subject yielding 64 sequences in total. The proposed algorithm was applied to all 3200 *in-vivo* lung ultrasound images. The results showed that the average number of B-lines was 0.28±0.06 (Mean±Std) in scans belonging to the patients compared to 0.03±0.06 (Mean±Std) in the healthy subjects. Also, the Mann-Whitney test showed a significant difference between the two groups with p-value of 0.015, and indicating that the proposed algorithm was able to differentiate between the healthy volunteers and the patients. In conclusion, the method can be used to automatically and to quantitatively characterize the distribution of B-lines for diagnosing pulmonary edema.**

***Index Terms*—B-lines, segmentation, pulmonary edema, ultrasound imaging**

I. Introduction

Lung ultrasound (LUS) has received increasing attention in recent years, as it enables a quick visual evaluation of the lung tissue and pleura without imposing radiation [1]. B-lines are important ultrasound artifacts used in LUS for detection of pulmonary disease. They are defined as discrete laser-like vertical hyperechoic reverberation artifacts that arise from the pleura, spread down without fading to the edge of the screen, and move synchronously with lung sliding [2].

An intimate mixture of air and water characterizes the lung state. Change in their balance can be a sign of pulmonary disease. Interactions of water and air in ultrasound lung scans generate a variety of artifacts, and a LUS image of pulmonary disease is therefore based on analyzing these artifacts during visualization of the structures [3], [4], [5], [6]. B-lines are reverberation artifacts generated by multiple reflections of the ultrasound beam trapped between air- and water-rich structures. They originate from the visceral pleura (serous membrane covering the surface of the lungs) and spread down to the edge of the screen. B-line detection is essential in the assessment of lung-edema in LUS imaging, which is often present in patients with heart and lung diseases as well as patients having undergone major surgery [5], [7], [8]. B-lines are also seen in patients with interstitial lung diseases and have been used to grade disease severity [9]. In daily clinical practice, patients suspected for pulmonary edema are imaged with X-ray, and often repeatedly imaged with short intervals to monitor the effect of the applied treatment. Lung ultrasound is a well-established modality, but it is often bypassed, as the medical staff handling these patients are not familiar with the method.

In 1997, Lichtenstein [10] showed a correlation between B-lines in ultrasound, and chest computed tomography (CT) with edema. Even though LUS already had been used for evaluation of pleural effusion, it was the first time that the diagnostic value of B-line artifacts was shown. In 2004, Picano [11] showed the correlation between the number of B-lines detected by LUS and X-ray findings for assessing the presence of extra-vascular lung water (EVLW). Since then, multiple studies have shown the methodological validation and clinical application of B-lines for diagnosing pulmonary diseases. The common practice for diagnosing pulmonary edema with ultrasound is based on visual analysis and interpretation of B-lines [4], [5], [6], [12].

Several B-lines distributed bilaterally in more scans on each lung defines diffuse alveolar-interstitial syndrome (caused by hydrostatic pulmonary edema, lesional pulmonary edema or fibrosis) [5]. The standard pathological routine for diagnosing this disease is to investigate the number of B-lines in a single scan or frame. A study performed by intensivists showed that the mean distance between two adjacent B-lines at the lung surface is never more than 7 mm, and this should be the widest distance between B-lines to be significant [3]. Another study used the criteria of counting at least three artifacts with a distance between adjacent lines of no more than 7 mm for identifying edema [13]. On the other hand, visualization of isolated B-lines, or visualization of multiple B-lines of more than 7 mm apart in a single scan, was considered a normal finding [13]. Major factors affecting the accuracy of the examination are interpretation error due to inexperience and habituation. Computer-assisted interpretation can potentially address the issue of these errors, and facilitate the adoption by users.

A large multicenter study (n=1005) examined with a six-zone scanning protocol the presence of B-lines. The LUS appoach had a significantly higher accuracy in differentiating acute decompensated heart falure from noncardiac causes of acute

This article has been accepted for publication in a future issue of this journal, but has not been fully edited. Content may change prior to final publication. Citation information: DOI 10.1109/TUFFC.2018.2885955, IEEE Transactions on Ultrasonics, Ferroelectrics, and Frequency Control

dypnea when compared with clinical evaluation and chest radiography [14]. Another large prospective study (n=788) was conducted for point-of-care ultrasonography [15]. Using LUS, improved diagnosing and faster treatment were given to the patients group treated with point-of-care ultrasonography compared with the control group.

A systematic review study was conducted in 2014, with primary objective of determining the sensitivity and specificity of ultrasound using B-lines in diagnosing acute cardiogenic pulmonary edema (ACPE) in patients presenting to the emergency department with acute dyspnea [16]. The authors included 7 prospective cohort and prospective case-control studies that recruited patients presenting to hospital with symptomatic, acute dyspnea, or where there was a clinical suspicion of congestive heart failure, and reported the sensitivity and specificity of B-lines in diagnosing ACPE. The results showed that sensitivity of US using B-lines to diagnosis ACPE is 94.1% and the specificity is 92.4%. The results showed the importance of point-of-care lung ultrasound has shown promise as a diagnostic tool in this setting.

Apart from the recent advances in application of lung ultrasound, very few automated techniques for characterizing the B-line artifacts and pulmonary disease is presented in the literature. In 2013 a technique for B-line scoring was presented [17]. The technique used a polar reformatting technique to convert the images to a 60×40 rectangular grid, and extracted 5 features from each column to detect the B-lines.

Moshavegh [18] presented an automated technique for detecting and characterizing B-lines. The technique first delineated the pleura on the scan using graphs, and then detected and visualized the B-lines on the B-mode. A computer-aided quantitative method for detection of pulmonary edema in mechanically ventilated cardiac surgery patients was presented in 2016 [19]. The technique analysed the mean and standard deviation of grayscale changes in B-mode images to identify edema. Another study used Hough transform for detcting B-lines [20]. The study compared the Hough transform algorithm with other automated techniques, as well as the previously presented technique by authors of this paper in [18].

The main purpose of this paper is to proposes an automatic method for accurate detection and visualization of B-lines in ultrasound lung scans, which provides a quantitative measure for the number of B-lines present. Section II introduces the proposed algorithm. Section III introduces the scanning protocol, and section IV presents the ultrasound data used in this study. Section V presents the preliminary *in-vivo* results. Section VI discusses the findings, and section VII concludes the paper.

II. Materials and Methods

B-lines are reverberation artifacts that originate from water-thickened pulmonary interlobular septa [7]. Fig. 1 shows the anatomy of secondary lobule, in which the interlobular septum is thickened due to the existence of fluid. In ultrasound images of lungs, B-lines originate from the visceral pleural line and extend to the edge of the display, and Fig. 2 illustrates how B-lines are generated in ultrasound.

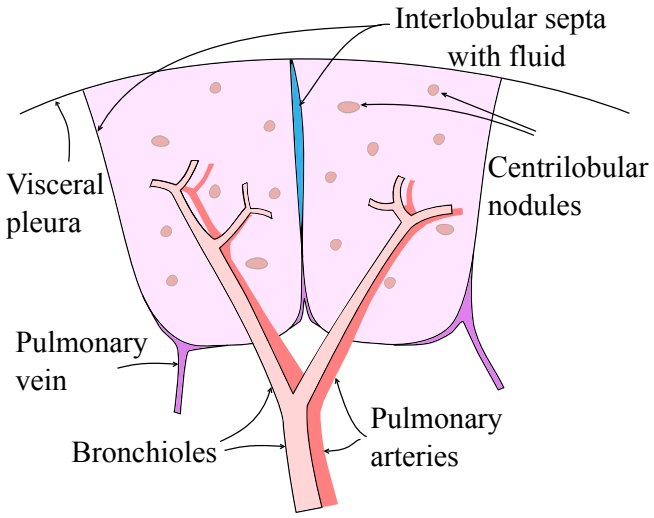

Fig. 1: Anatomy of the secondary lobule and its components. The interlobular septum is thickened due to the existence of fluid.

The purpose of the algorithm is two folded, first to automatically detect the B-lines, and second to characterize the distribution of B-lines to discriminate between healthy volunteers and patients with pulmonary edema. The proposed method contains five distinct steps. First, the pleural line is delineated using a random walks method [21]. Second, the upper-pleural region is excluded from the scan, and the B-line artifacts are identified on the scan plane. Third, an alternate sequential filtration is applied to the results of step 2 to better highlight the B-lines. Fourth, the result of step 3 is top-hat filtered to make sure that B-lines are laterally detached. Finally, a Gaussian model is fitted to each detected B-line, and the peak point of the fitted Gaussian models corresponding to the B-lines are calculated and used to determine the position of B-lines. B-lines are then overlaid on the B-mode image. The five main steps of the algorithm are discussed in detail in this section.

Step 1. Pleural line delineation

The first essential step in detection of B-lines is to delineate the pleural line on the lung scans. For this purpose, a graph based approach that computes a per-pixel uncertainty map based on the information depicted by an ultrasound image was used [22]. This method measures the uncertainty in attenuated and/or shadow regions, and generates a normalized gray scale map that can be used for delineation of different structures in ultrasound images. To identify the map for each ultrasound frame, a random walks framework was used that takes into account ultrasound specific constraints [22]. The solution of the random walks equilibrium problem is global and takes the entire content of the RF data into account. The required starting points were automatically placed at the beginning of each scan-line to represent the transducer elements. Thus, a problem was formulated by computing the probability of a

This article has been accepted for publication in a future issue of this journal, but has not been fully edited. Content may change prior to final publication. Citation information: DOI 10.1109/TUFFC.2018.2885955, IEEE Transactions on Ultrasonics, Ferroelectrics, and Frequency Control

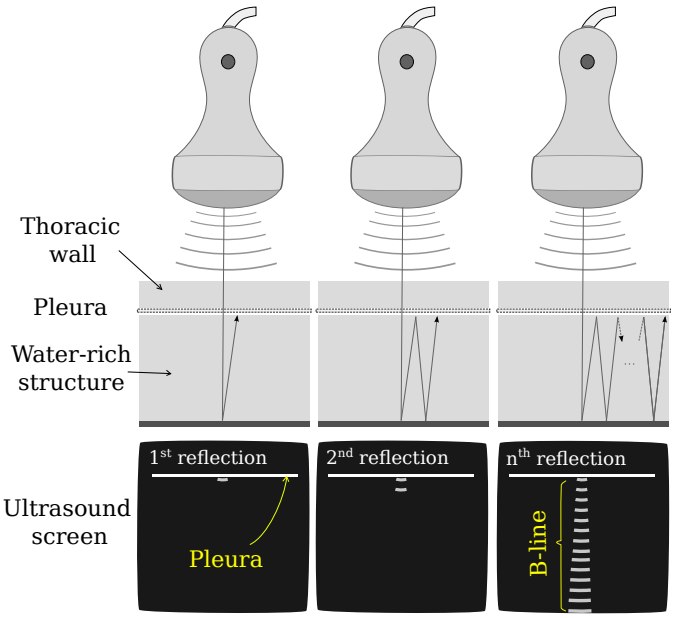

Fig. 2: Illustration of how B-lines are generated. They are hyperechoic reverberation artifacts arising from the pleural line and spreading down towards the lower edge of the screen.

random walk starting from a pixel to reach the transducer elements. The domain specific knowledge for ultrasound was integrated with a simple modeling of the ultrasound image formation process. The ultrasound specific constraints obtained from physics of acquired RF data by the transducer must be integrated to ensure the accuracy of the confidence map. One of the fundamental properties of ultrasound is the attenuation of the signal by increasing depth. The Beer–Lambert Law was used to express the depth dependent attenuation, and the attenuated signal I could be given by $I = I_0 \exp(-\alpha d)$, where I_0 is the initial intensity, α the attenuation coefficient, and d the distance from the source. This property was included into the confidence map in a way that the further away a random walk starts from the transducer, the more unlikely it will be able to reach one of the transducer elements. The computed confidence map presents a depth dependent attenuation, in which the low probabilities represent high attenuation and vise versa. The maps generated for ultrasound lung images depict a clear distinction along the pleural line due to the abrupt change in the attenuation. Therefore, the map was used to delineate the pleura, and determine the upper-pleural region to exclude that from the RF-data prior to detecting the B-lines (see Fig. 3b). The pleural line was delineated on the confidence map by thresholding. The region with values bigger than the global threshold of entire map was considered the upper pleura, and the remaining was the lower pleural region.

Step 2. B-line detection

B-line detection contains four steps. First, the area on the scan corresponding to the upper-pleura was excluded from the data (Fig. 3c), and the B-lines were characterized from the remaining of the RF-data. This was done because B-lines originate from the pleura and extend downwards to the end of the screen. Second, to extract the vertical edges in the RF-data, a normalized cumulative histogram the remained RF-data was computed axially. This yielded an axial-cumulative image, in which each column was the cumulative sum of the corresponding scan-line in the RF-data (Fig. 3d). Each column of the axial-cumulative image was normalized to the maximum brightness of the same column. Third, this image was inverted, and an adaptive histogram equalization was performed to increase the contrast (Fig. 3e). Finally, a binary mask including regions with gray scale values higher than 0.5 inside the histogram-equalized image was generated (Fig. 3f). This binary mask outlines the most prominent B-lines in the envelope data. The procedure is detailed in Algorithm 1. This mask is further optimized in the following steps to better characterize and visualize the B-lines.

Step 3. B-lines axial improvement

The binary mask generated in the step 2 and shown in Fig. 3f, provides a very crude characterization of B-lines. An alternate sequential filtering (ASF) procedure using a repeated sequential morphological opening and closing was applied to the mask [23]. ASF closes small gaps axially and isolates the objects laterally. The procedure is explained in Algorithm 2. ASF highlights the vertical B-lines and isolate them from each other laterally. Fig. 3g is the result of ASF, in which the B-lines are better identified in comparison with those in Fig. 3f. An axial line-structuring element along the ultrasound beam, was used for ASF filtering. This was used to ensure that only elongated and axial information (B-line artifacts) in the compressed data is preserved and highlighted.

Step 4. B-lines latteral separation

The generated mask in the previous step contains prominent axially elongated and adjacent tails, which locate the B-lines. However, the tails can be laterally connected, which deteriorates the clean separation of B-lines. To separate and extract the B-lines automatically, a top-hat transformation was used. The top-hat transformation originally proposed by Mayer [24] is a mathematical morphology operator that uses morphological opening or closing for extracting bright (respectively dark) objects from an uneven background in a 2D grey-scale image. Top-hat transformation can be formulated in two ways: white top-hat (WTH) and black top-hat (BTH). WTH can also be used to identify prominent peaks in a 1D signal, and the BTH as the dual of the WTH can be used to identify the prominent minima in a 1D signal. In this study, a (WTH) with a flat disk structuring element was used to extract the B-lines. The WTH transformation of a 1D signal f with a flat structuring element B is defined as $T_{white}(f) = f - (f \circ B)$.

To identify the actual B-lines, the top-hat transform was applied using a line structuring element (B) that was longer than the size of the connected regions. The $\circ$ is the opening operator and is a min operation that removes the regions smaller than the size of structuring element. Subtracting this signal from the original signal produces a signal that only contains

This article has been accepted for publication in a future issue of this journal, but has not been fully edited. Content may change prior to final publication. Citation information: DOI 10.1109/TUFFC.2018.2885955, IEEE Transactions on Ultrasonics, Ferroelectrics, and Frequency Control

Algorithm 1 B-line detection

Input: RF, RF-data acquired from the scanner.

Output: Binary mask (B_{bl}) highlighting strong axial B-lines.

procedure B-LINE DETECTION
  $Env = \log_{10}(|Hilbert\{RF\}|)$ # performing the Hilbert transformation, and computing the envelope of RF data.
  Let $Ax\_cdf(M,N)$ be a discrete gray scale image denoting the axial cumulative image of the envelope data with M rows and N columns.
  for each $i \in M$ **do**
    for each $ii \in N$ **do**
      $Ax\_cdf(i,ii) = \frac{\sum_{j=0}^{i} Env(j,ii)}{max(Env(ii).col)}$ # computing the axial cumulative sum and normalizing to the maximum intensity of that column.
    end for
  end for
  $B_c = max(Ax\_cdf) - Ax\_cdf$ # inverting the axial cumulative image.
  $B_c = adapthisteq(B_c)$ # function performing the adaptive histogram equalization.
  Let B_c be a discrete gray scale image and let n_i be the number of occurrences of gray level i.
  $p_{B_c(i)} = p(B_c = i) = \frac{n_i}{n}, 0 < i < L$ # probability of an occurrence of a pixel of level i in the image.
  Let L be the total number of gray levels in the image (in our case 256), n being the total number of pixels in the image, and $p_{B_c(i)}$ be the image's histogram for pixel value i, and normalized to $[0,1]$.
  for each $i \in L$ **do**
    $cdf_{B_c(i)} = \sum_{j=0}^{i} p_{B_c(j)}$ # define the cumulative distribution function corresponding to p_{B_c}.
  end for
  Let th_l be the gray value for which $cdf_{B_c=0.5}$ and th_h be the gray value in which $cdf_{B_c=1}$.
  Let B_{bl} be a zero binary mask with the same size as image B_c
  for each $ii \in N$ **do** # N is the total number of pixels in the image B_{bl}.
    if $th_l < B_c(ii) < th_h$ **then**
      $B_{bl}(ii) = 1$
    end if
  end for
end procedure

Algorithm 2 Alternate sequential filtering

Input: B_{in} Binary mask outlining most prominent edges in RF-data, and N maximum size of the structuring element in ASF that can vary according to the number of samples in RF-data in axial direction.

Output: B_{ASF} Binary mask in which the strong axial B-lines are highlighted.

procedure ASF
  $B_{ASF} = B_{in}$
  for each $i \in N$ **do**
    Let S_{lin} be a line structuring element of length N [23].
    $B_{ASF} = (B_{ASF} \ominus S_{lin}) \oplus S_{lin}$ # performing the morphological opening.
    $B_{ASF} = (B_{ASF} \oplus S_{lin}) \ominus S_{lin}$ # performing the morphological closing.
  end for
end procedure

Note: $\oplus$ and $\ominus$ denote morphological dilation and erosion respectively [23].

the desired strong peaks. Fig. 3h shows B-lines detected after top-hat filtering for a lung scan of a healthy subject.

Step 5. Gaussian model fitting

The B-lines curve after top-hat filtering was quite rough, and the peak points of the B-lines were not well-defined. A Gaussian model was fitted to each B-line (Fig. 3i). The peak points of the Gaussian models were calculated and considered to be the position of the B-lines along the pleura. The final Gaussian-fitted B-line mask was then overlaid on the B-mode. This is done to provide a visual inspection of B-lines in lung ultrasound, and to assist doctors in their diagnosis.

Figs. 5 and 6 show two examples of the detected pleura and B-lines on lung scans of a patient and a healthy subject respectively. show two examples of the detected pleura and B-lines on lung scans of a patient and a healthy subject respectively.

III. SCANNING PROTOCOL

This study was performed after approval by the National Committee on Biomedical Research Ethics (no. 16031001).

This article has been accepted for publication in a future issue of this journal, but has not been fully edited. Content may change prior to final publication. Citation information: DOI 10.1109/TUFFC.2018.2885955, IEEE Transactions on Ultrasonics, Ferroelectrics, and Frequency Control

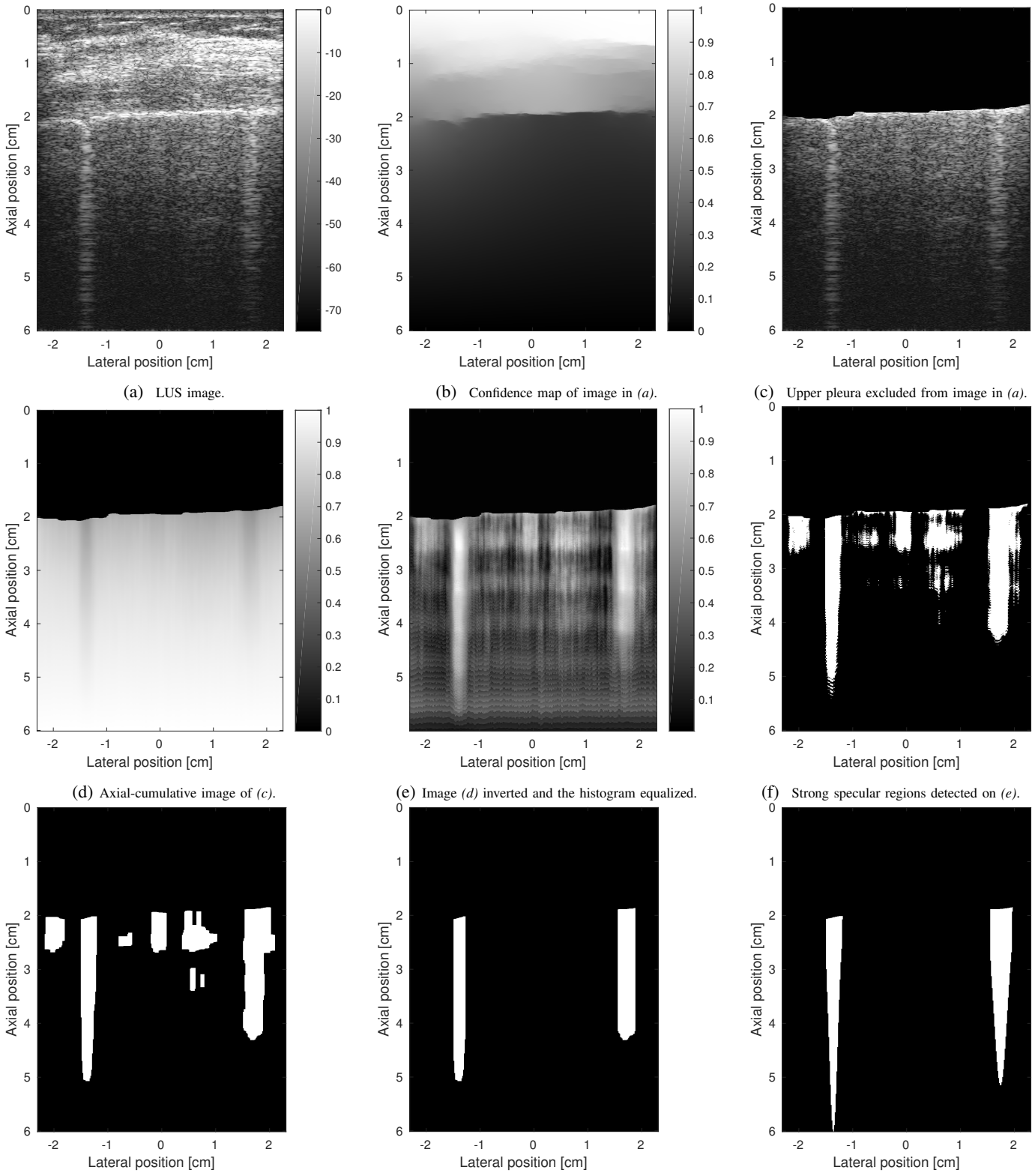

(a) LUS image.

(b) Confidence map of image in *(a)*.

(c) Upper pleura excluded from image in *(a)*.

(d) Axial-cumulative image of *(c)*.

(e) Image *(d)* inverted and the histogram equalized.

(f) Strong specular regions detected on *(e)*.

(g) Result of ASF.

(h) Result of top-hat.

(i) Result of Gaussian fitting.

Fig. 3: Automatic B-line detection performed on a LUS scan of a patient with pulmonary edema.

This article has been accepted for publication in a future issue of this journal, but has not been fully edited. Content may change prior to final publication. Citation information: DOI 10.1109/TUFFC.2018.2885955, IEEE Transactions on Ultrasonics, Ferroelectrics, and Frequency Control

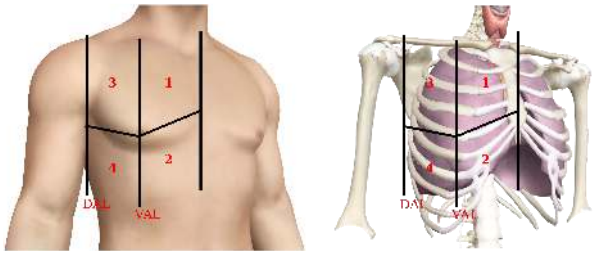

Fig. 4: 8-zone scanning protocol. Chest was divided into 8 zones (4 per hemithorax), for each of which the intercostal spaces were examined for B-lines and the best scan is recorded (one scan per zone).

The proposed algorithm was applied to *in-vivo* ultrasound lung scans acquired from healthy subjects and patients after informed consent. An eight-zone scanning protocol was used for acquiring ultrasound lung scans as recommended by others [2], [25]. The ultrasound examination consisted of bilateral scanning of the ventral and dorsal chest walls performed on each subject in cranial and caudal positions (Fig. 4). The probe was placed in the intercostal space parallel to the ribs to obtain a window of the pleural line without shadowing from the ribs. Chest was divided into 8 zones (4 per hemithorax), for each of which the intercostal spaces were examined for B-lines and the best scan is recorded (one scan per zone). The 8-zone scan approach was employed to examine the lungs as thorough as possible in supine hospitalized patients. Fig. 4 shows where on the subjects examination was performed.

IV. Ultrasound dataset

Four healthy subjects and four patients with pulmonary edema were scanned. The patients had undergone major cardiac surgery. The healthy subjects were four males of 32, 42, 31 and 28 year-old. The first patient was a 67 year-old male, who have had coronary artery bypass grafting (CABG) for stenotic coronary arteries (abnormal narrowing in 3 vessels). The second patient was a 44 year-old female, who have had surgery for myxoma (benign tumor) in the left atrium. The pulmonary edema in this patient was mainly due to extracorporeal circulation via heart-lung machine. The third patient was a 83 year-old male, who have had CABG surgery for stenotic coronary arteries (abnormal narrowing in 3 vessels). Finally, the fourth patient was a 68 year-old male, who have had surgical implantation of a heart-mate (mechanical heart) because of cardiomyopathy. All four patients were under mechanical ventilation, and were scanned 24 hours after surgeries performed.

A coarse method to infer the level of edema was to measure the ratio of The alveolar partial pressure of oxygen (PO_2) to fraction of inspired gas that is oxygen (FiO_2). The $\frac{PO_2}{FiO_2}$ ratio measures the difference between the amount of oxygen in the blood, and the amount of oxygen that is inhaled while breathing. This test measures the extent of decreased lung function [26], [27]. PO_2, FiO_2, and $\frac{PO_2}{FiO_2}$ ratio for the patients via mechanical ventilation is depicted in Table I.

The beamformed RF data were acquired with a BK3000 ultrasound scanner (BK Ultrasound, Denmark) driving a 5.5 MHz linear transducer (BK Ultrasound, Denmark), scanning down to 6 cm without compounding. The compounding was deactivated given the fact that compounding different shots with different angles was lowering the brightness of the B-line artifacts.

Descriptive statistics were computed along with an 2-tailed Mann-Whitney test for examining the difference between the two groups with $p < 0.05$ considered significant. SPSS 22 (IBM, Armonk, NY, USA) was used for all statistical analyses.

V. Results

The average number of B-lines was calculated for each subject across 8 scans recorded from a subject. The results are shown in Table I. In this study a linear transducer with 4 cm lateral footprint was used. The designed feature was able to differentiate between the healthy and unhealthy classes. The average number of B-lines was 0.28±0.06 (Mean±Std) in scans belonging to the patients. On the other hand, in the healthy subjects, average number of B-lines was 0.03±0.06 (Mean±Std). The Mann-Whitney test showed a significant difference between the two groups with p-value of 0.015.

VI. Discussion

The preliminary in vivo study using the proposed algorithm for automatic B-line detection was applied to 64 acquired lung sequences (3200 frames) acquired from 4 healthy volunteers and 4 patients 24 hours after cardiac surgery. The proposed algorithm used all data in a sequence and not single frames, as in conventional lung ultrasound, for B-line detection. Figs. 5 and 6 show two examples of the detected pleura and B-lines on lung scans of a patient and a healthy subject respectively. The standard routine for diagnosing pulmonary disease is to identify the distribution of B-lines in a single scan or frame [5]. To detect edema in cine-loops of ultrasound lung scans and to discriminate between healthy volunteers and patients with pulmonary edema, the average number of detected B-lines for each patient was used.

The results of the study showed that the proposed algorithm was able to detect the B-lines on ultrasound scans, and was able to distinguish healthy volunteers form patients with lung edema by the average number of B-lines. The proposed method can potentially be used as an automated tool to differentiate between scans belonging to patients and healthy subjects.

Results of the study also showed that in some scan views of the patients, no B-lines were detected. It is because B-lines were generated where edema was initiated, and not all 8 views scanned from a subject presented edema. This emphasizes the need for thorough ultrasound examination of lungs in these types of patients as edema is not evenly distributed. Thus, a thorough ultrasound examination of the lungs as performed in this study is important when assessing B-lines.

Chest x-ray does not provide a quantification for pulmonary edema and is not the best modality for detection of pulmonary

This article has been accepted for publication in a future issue of this journal, but has not been fully edited. Content may change prior to final publication. Citation information: DOI 10.1109/TUFFC.2018.2885955, IEEE Transactions on Ultrasonics, Ferroelectrics, and Frequency Control

TABLE I: NUMBER OF B-LINES DETECTED FOR ALL SUBJECTS.

Measures / Subjects	Age (years)/ Gender	Health issue	FiO_2 [%]	PO_2 $[mmHg]$	$\frac{PO_2}{FiO_2}$ $[mmHg]$	Views in which B-lines observed and # of B-lines	Average # of B-lines
Patient 1	67 / male	Stenotic coronary arteries (3 vessels)	40	100.5	251.25	View 8 (2 B-lines)	0.25
Patient 2	44 / female	Myxoma (benign tumor) in the left atrium	70	147.76	211.08	View 3 (1 B-line) and View 6 (1 B-line)	0.25
Patient 3	83 / male	Stenotic coronary arteries (3 vessels)	50	80.25	160.5	View 5 (1 B-line) and View 6 (1 B-line)	0.25
Patient 4	68 / male	Cardiomyopati (cardiac muscle disease)	65	165.01	253.86	View 3 (2 B-lines) and View 6 (1 B-line)	0.375
Volenteer 1	32 / male	–	–	–			0
Volenteer 2	42 / male	–	–	–			0
Volenteer 3	31 / male	–	–	–			0
Volenteer 4	28 / male	–	–			View 7 (1 B-line)	0.125

edema even though it is modality most often chosen due to availability [5], [7]. Chest x-ray is a ionizing modality, which is harmful for cellular DNA, while ultrasound is harmless. Also, chest x-ray imaging is a service offered by the radiology department, while lung ultrasound is performed bedside by staff.

The proposed automated algorithm automatically identify the distribution of B-lines. The algorithm can potentially be used in daily clinical practice as a tool for making a quantitative estimation of pulmonary edema as it provides a quantitative measure for B-lines presence.

One study compared the Hough transform algorithm with other automated B-line detection techniques [20]. A reduced version of the presented technique by Moshavegh [18] is implemented and used for comparison by Anantrasirichai [20].It implemented the step 3 only, which was the alternate sequential filtering (ASF). Therefore, the comparison was rather based on a partial implementation of the original algorithm.

In this study, 4 patients and 4 healthy subjects were examined. The future study holds a larger data set of patients with different levels of edema with followup scans. This could be of clinical interest, as the performance of the algorithm could be evaluated in differentiating between scans belonging to the patients with different levels of edema. Also the recovery of edema in follow-up scans should result in lower average number of B-lines.

In this study, the PO_2 and FiO_2 values were only measured for patients. Another study reported PO_2 at around $80 - 100\ mmHg$ and $FiO_2 = 21\%$ for healthy adult subjects. These values result in $\frac{PO_2}{FiO_2} = 400\ mmHg$ for healthy subjects [28]. The North American-European Consensus Conference, also defined acute lung injuries (ALI) in 1994 [26].They defined $\frac{PO_2}{FiO_2}$ values lower than $300\ mmHg$ as acute hypoxemia. Hypoxemia is an abnormally low level of oxygen in the arterial blood, and has many causes such as respiratory disorders [26]. The $\frac{PO_2}{FiO_2}$ values measured for all four patients in our study were less than $300\ mmHg$, thus patients suffered from hypoxemia.

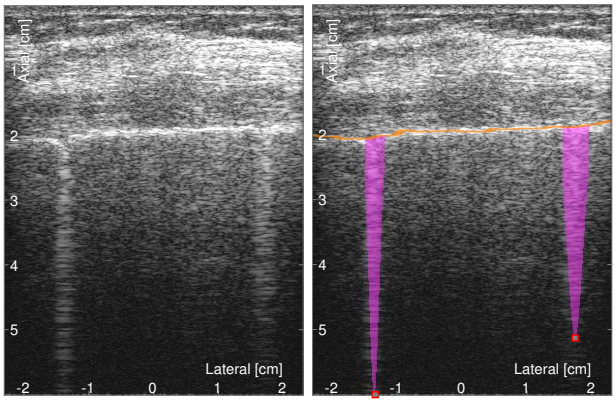

(a) LUS scan containing two B-lines.

(b) Pleural line is outlined and two B-lines are detected in *(a)* and overlaid.

Fig. 5: Lung scan of a patient after surgery, for which the pleural line is outlined, and two B-lines are detected.

Some limitations of the study should be mentioned. As only 8 subjects were scanned, a larger study is warranted. No inter- or intra-observer variation were assessed. A larger data set is of course needed for drawing any clinical conclusion. Authors considering a larger study, in which patients with different grades of edema are scanned by more than one user. The aim would be also to have follow-up scans to investigate whether the number of b-lines and subsequently edema reduces. The inter- and intra-observer variance can therefore be investigated.

The B-line algorithm was not calculated real-time, hence, no B-line estimate was given directly on the scanner. However, the measure is not computationally demanding, and a real-time implementation could be realized on a commercial scanner.

This article has been accepted for publication in a future issue of this journal, but has not been fully edited. Content may change prior to final publication. Citation information: DOI 10.1109/TUFFC.2018.2885955, IEEE Transactions on Ultrasonics, Ferroelectrics, and Frequency Control

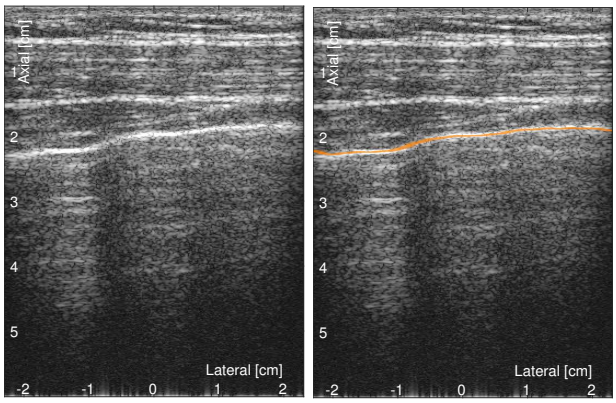

(a) LUS scan containing no B-lines.

(b) Pleural line is outlined and no B-lines are detected in *(a)*.

Fig. 6: Lung scan of a healthy subject, for which the pleural line is outlined, and no B-lines are detected.

VII. Conclusion

This paper presented a novel automatic B-line detection algorithm. It automatically finds B-lines using sequences of lung ultrasound. The results indicated the proposed technique was able to detect the B-lines and was able to differentiate the ultrasound scans acquired from the patients after cardiac surgery and those acquired from healthy subjects. The proposed method enables an automatic quantitative estimation of edema and may have a substantial clinical value.

References

[1] C. F. Dietrich, G.Mathis, M. Blaivas, G. Volpicelli, A. Seibel, D. Wastl, N. S. S. Atkinson, X. W. Cui, M. Fan, and D. Yi, "Lung b-line artefacts and their use," *Journal of Thoracic Disease*, vol. 8, no. 6, pp. 1356–1365, 2016.

[2] G. Volpicelli, M. Elbarbary, M. Blaivas, D. L. A., G. Mathis, A. W. Kirkpatrick, L. Melniker, L. Gargani, V. E. Noble, G. Via, A. Dean, and J. W. Tsung, "International evidence-based recommendations for point-of-care lung ultrasound," *Intensive Care Medicine*, vol. 38, no. 4, pp. 577–591, 2012.

[3] D. Lichtenstein, G. Meziere, P. Biderman, and A. Gepner, "The comet-tail artifact: An ultrasound sign ruling out pneumothorax," *Intensive Care Med.*, vol. 25, no. 4, pp. 383–388, 1999.

[4] E. Agricola, T. Bove, M. Oppizzi, G. Marino, A. Zangrillo, A. Margonato, and E. Picano, "Ultrasound comet-tail images: A marker of pulmonary edema: A comparative study with wedge pressure and extravascular lung water," *Chest*, vol. 127, no. 5, pp. 1690–1695, 2005.

[5] G. Volpicelli, A. Mussa, G. Garofalo, L. Cardinale, G. Casoli, F. Perotto, C. Fava, and M. Frascisco, "Bedside lung ultrasound in the assessment of alveolar-interstitial syndrome," *Am. J. Emerg. Med.*, vol. 24, no. 6, pp. 689–696, 2006.

[6] L. Gargani, F. Frassi, G. Soldati, P. Tesorio, M. Gheorghiade, and E. Picano, "Ultrasound lung comets for the differential diagnosis of acute cardiogenic dyspnoea: A comparison with natriuretic peptides," *Eur. J. Heart Failure*, vol. 10, no. 1, pp. 70–77, 2008.

[7] L. Gargani, "Lung ultrasound: A new tool for the cardiologist," *Cardiovascular ultrasound*, vol. 9, no. 1, 2011.

[8] D. A. Lichtenstein, "Lung ultrasound in the critically ill," *Ann Intensive Care*, vol. 4, no. 1, 2014.

[9] A. Hasan and H. Makhlouf, "B-lines: Transthoracic chest ultrasound signs useful in assessment of interstitial lung diseases," *Annals of Thoracic Medicine*, vol. 9, no. 2, pp. 99–103, 2014.

[10] D. Lichtenstein, G. Mézière, P. Biderman, A. Gepner, and O. Barré, "The comet-tail artifact. an ultrasound sign of alveolar-interstitial syndrome," *Am. J. Respir. Crit. Care. Med.*, vol. 156, no. 5, pp. 1640–1646, 1997.

[11] Z. Jambrik, S. Monti, V. Coppola, E. Agricola, G. Mottola, M. Miniati, and E. Picano, "Usefulness of ultrasound lung comets as a nonradiologic sign of extravascular lung water," *Am. J. Cardiology*, vol. 93, no. 10, pp. 1265–1270, 2004.

[12] L. Gargani, V. Lionetti, C. D. Cristofano, G. Bevilacqua, F. Recchia, and E. Picano, "Early detection of acute lung injury uncoupled to hypoxemia in pigs using ultrasound lung comets," *Crit Care Med.*, vol. 35, no. 12, pp. 2769–2774, 2007.

[13] G. Volpicelli, L. Cardinale, G. Garofalo, and A. Veltri, "Usefulness of lung ultrasound in the bedside distinction between pulmonary edema and exacerbation of COPD," *Am. Soc. Emerg. Radiol.*, vol. 15, no. 3, pp. 145–151, 2008.

[14] E. Pivetta, A. Goffi, E. Lupia, M. Tizzani, G. Porrino, E. Ferreri, G. Volpicelli, P. Balzaretti, A. Banderali, A. Iacobucci, S. Locatelli, and G. Casoli, "Lung ultrasound-implemented diagnosis of acute decompensated heart failure in the ed," *Chest*, vol. 148, no. 1, pp. 202–210, 2015.

[15] C. B. Laursen, E. Sloth, A. T. Lassen, R. d. Christensen, J. Lambrechtsen, P. H. Madsen, D. P. Henriksen, J. R. Davidsen, and F. Rasmussen, "Point-of-care ultrasonography in patients admitted with respiratory symptoms: a single-blind, randomised controlled trial," *The Lancet Respiratory Medicine*, vol. 2, no. 8, pp. 638–646, 2014.

[16] M. A. Deeb, S. Barbic, R. Featherstone, J. Dankoff, and D. Barbic, "Point-of-care ultrasonography for the diagnosis of acute cardiogenic pulmonary edema in patients presenting with acute dyspnea: A systematic review and meta-analysis," *Academic Emergency Medicine*, vol. 21, no. 8, pp. 843–852, 2014.

[17] L. J. Brattain, B. A. Telfer, A. S. Liteplo, and V. E. Noble, "Automated B-line scoring on thoracic sonography," *J. Ultrasound Med.*, vol. 32, no. 12, pp. 2185–2190, 2013.

[18] R. Moshavegh, K. L. Hansen, H. M. S. M. C. Hemmsen, C. E. andv M. B. Nielsen, and J. A. Jensen, "Novel automatic detection of pleura and B-lines (comet-tail artifacts) on in vivo lung ultrasound scans," in *Proc. SPIE Med. Imag.*, vol. 9790, 2016, pp. 97 900K–97 900K–7.

[19] F. Corradi, C. Brusasco, A. Vezzani, G. Santori, T. Manca, L. Ball, F. Nicolini, T. Gherli, and V. Brusasco, "Computer-aided quantitative ultrasonography for detection of pulmonary edema in mechanically ventilated cardiac surgery patients," *Chest*, vol. 150, no. 3, pp. 640–651, 2016.

[20] N. Anantrasirichai, W. Hayes, M. Allinovi, D. Bull, and A. Achim, "Line detection as an inverse problem: Application to lung ultrasound imaging," *IEEE Trans. Med. Imag.*, vol. 36, no. 10, pp. 2045–2056, 2017.

[21] L. Grady, "Random walks for image segmentation," *IEEE. Trans Patt. Ana. Mach. Int.*, vol. 28, no. 11, pp. 1768–1783, Nov 2006.

[22] A. Karamalis, W. Wein, T. Klein, and N. Navab, "Ultrasound confidence maps using random walks," *Med. Image Anal.*, vol. 16, no. 6, pp. 1101–1112, 2012.

[23] R. C. Gonzalez and R. E. Woods, *Digital Image Processing*, 3rd ed. Upper Saddle River, NJ, USA: Prentice-Hall, Inc., 2006.

[24] F. Meyer, "Contrast features extraction, special issues of practical metallography," in *Quant. Anal. Microstruct. Mat. Sc. Bio. Med.*, vol. 8, 1977.

[25] S. Coiro, p. Rossignol, G. Ambrosio, E. Carluccio, G. Alunni, A. Murrone, I. Tritto, F. Zannad, and N. Girerd, "Prognostic value of residual pulmonary congestion at discharge assessed by lung ultrasound imaging in heart failure," *European Journal of Heart Failure*, vol. 17, no. 11, pp. 1172–1181, 2015.

[26] G. R. Bernard, A. Artigas, K. L. Brigham, J. Carlet, K. Falke, L. Hudson, M. Lamy, J. R. Legall, A. Morris, and R. Spragg, "The american-european consensus conference on ards. definitions, mechanisms, relevant outcomes, and clinical trial coordination." *Am. J. Resp. Crit. Car. Med.*, vol. 149, no. 3, pp. 818–824, 1994.

[27] A. Fein, R. F. Grossman, J. G. Jones, E. Overland, L. Pitts, J. F. Murray, and N. C. Staub, "The value of edema fluid protein measurement in patients with pulmonary edema," *Am. J. Med.*, vol. 67, no. 1, pp. 32–38, 1979.

[28] A. Kratz, M. Ferraro, P. M. Sluss, and K. B. Lewandrowski, "Case records of the massachusetts general hospital. weekly clinicopathological exercises. laboratory reference values." *N. Engl. J. Med.*, vol. 351, no. 23, pp. 1548–1563, Oct 2004.